MECHANICAL ANALYSIS OF CARBON NANOTUBE/SHAPE MEMORY POLYMER COMPOSITES

Jinsu Kim[1], Yongsan An[1], Seokbin Hong[1] and Woong-Ryeol Yu[1*]

[1] Department of Materials Science and Engineering and Research Institute of Advanced Materials (RIAM), Seoul National University, Gwanak-ro 1, Gwanak-gu, Seoul 08826, Korea
(* E-mail: woongryu@snu.ac.kr)

Keywords: Shape memory polymer, Carbon nanotube, mechanical analysis, Constitutive equation

ABSTRACT

Shape memory polymers (SMPs) have some advantages such as large deformability, large recovery ratio, and lightweight compared to shape memory alloys. However, low stiffness and thermal conductivity are demerits. To overcome these limitations, carbon nanotube reinforced shape memory polymer composites (CNT-SMPCs) have been researched. In this study, experimental and numerical studies of CNT-SMPCs are carried out, aiming to provide a design method of the composites, in particular for aerospace applications. CNT-SMPCs are prepared using a SMP resin and multi-walled carbon nanotube(MWCNT). Tensile and stress relaxation tests are conducted using universal tensile machine with a heating chamber to characterize the mechanical properties of CNT-SMPCs. Using three-dimensional constitutive model, which was developed using multiplicative decomposition of the deformation gradient and shape memory strains, was used to simulate the SMP matrix inside CNT-SMPCs, while linear elastic model was used for CNTs. Using cohesive zone model, their interface was modelled. Finally, the effect of volume fraction and orientation of CNTs on the mechanical behaviour of CNT-SMPCs including shape memory properties is simulated.

1 INTRODUCTION

Shape memory polymers (SMPs) have some advantages such as large deformability, large recovery ratio, and lightweight. Because of these advantages, SMPs have been studied in various research fields as smart materials, e.g., biomedical and robtic actuators. However, there are some demerits, such as low stiffness and thermal conductivity, to apply to aerospace applications. To overcome these limitations, carbon nanotube reinforced shape memory polymer composites (CNT-SMPCs) have been researched.

To understand thermo-mechanical behavior of SMP at macro scale, many theoretical studies have been developed. Most developed multi-phase constitutive models are phenomenological models that describe the thermo-mechanical deformation behavior of SMPs using a continuum element [3,4]. To simulate the shape memory effect of SMP, Park et al. developed a three-dimensional constitutive equation using multiplicative decomposition of total deformation [1].

To predict the mechanical properties of CNT reinforced composites at micro scale, Dikshit et al. developed a microstructure level finite element model considering only CNT-phase and polymer-phase. The interface between CNT and polymer was assumed as perfect bonding. However, subsequent numerical and experimental results revealed that the mechanical properties of CNT reinforced composites is governed by the CNT-polymer interface because the interfacial shear strength is critical to the load transfer between CNT and polymer phase.

In this research, we investigate the mechanical behaviour of CNT-SMPCs using the 3D constitutive equation at macro and micro-level. Using multiplicative decomposition of the deformation gradient and shape memory strains, three-dimensional constitutive model was developed for shape memory polymers [1]. For macro-level simulation, CNT-SMPCs are considered as a continuum and their material parameters for the constitutive equation are determined using experiments and data extraction method which were reported in [1]. For micro-level simulation, CNTs and SMP are modelled individually and their mechanical behaviour is described by linear elastic law and aforementioned 3D constitutive model, respectively. The interface between CNT and SMP is modelled using cohesive zone model, of which the properties are determined so as to fit the macroscopic simulation and experiments. Then, the effect

of volume fraction and orientation of CNTs on the mechanical behaviour of CNT-SMPCs including shape memory properties is systematically investigated using simulation.

2 Mechanical analysis

2.1 Macro-level simulation

To analyze the thermomechanical behavior of SMPs and CNT-SMPCs, a constitutive model developed in a previous study was used [1]. This model consists of Mooney-Rivlin hyper elastic spring, Newtonian fluid and viscoplasticity elements as shown in Fig.1. The rubbery phase consists of Mooney-Rivlin spring and spring-dash pot element for analyzing viscoelastic behavior in high temperature condition, while the glassy phase contains additional viscoplastic element for non-recoverable deformation on glassy state and non-mechanical strain element for simulating shape memory strain. The volume fraction of these rubbery and glassy phases was determined by Helmholz free energy. Basic equations on each element are shown in Table.1. Details on the implementations of this constitutive equation will be discussed at the conference.

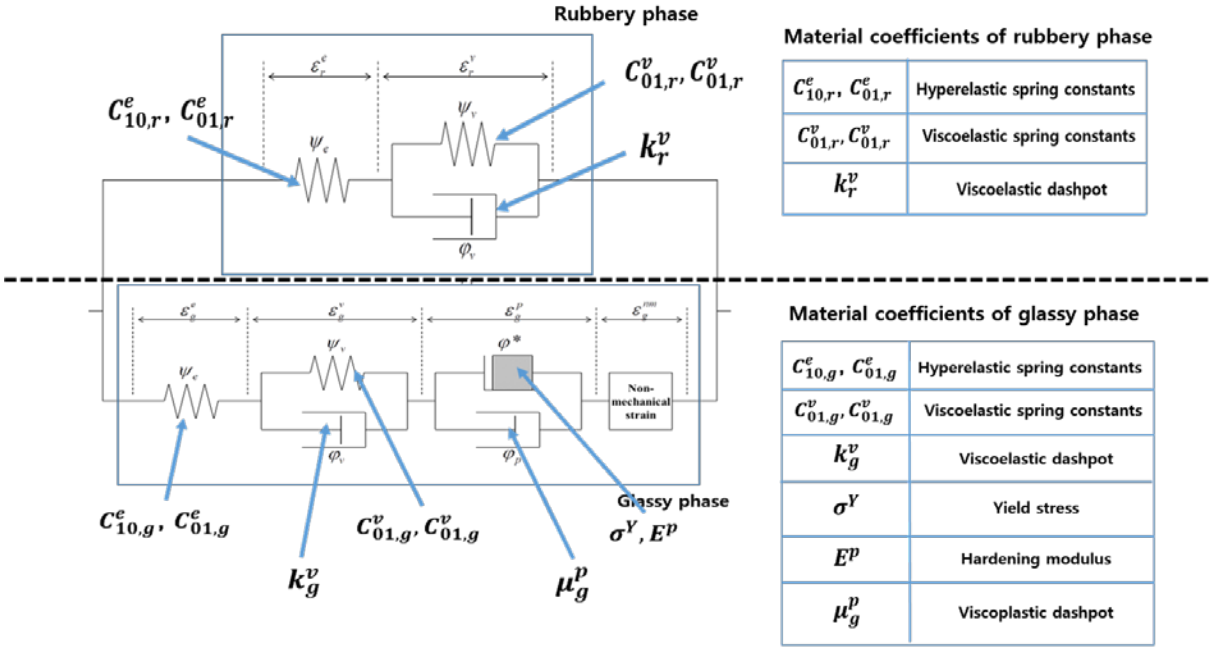

Figure 1: Phenomenological constitutive model for SMP and CNT-SMPC

Governing equation	
Mooney-Rivlin hyperelastic spring	$k_r \overset{\nabla}{\mathbf{C}}{}^v_r = f_{\mathbf{C}^v_r}\left(\mathbf{C}^v_r, \mathbf{F}, \mathbf{I}\right)$, $k_g \overset{\nabla}{\mathbf{C}}{}^v_g = f_{\mathbf{C}^v_g}\left(\mathbf{C}^v_g, \mathbf{F}, \mathbf{F}^p_g, \mathbf{F}^{nm}_g\right)$
Newtonian fluid	$\phi_r = \frac{1}{2} k_r \overset{\nabla}{\mathbf{C}}{}^v_r : \overset{\nabla}{\mathbf{C}}{}^v_r$
Viscoplasticity	$\overset{\nabla}{\mathbf{F}}{}^p_g = \frac{1}{k^p_g} \langle f \rangle \frac{\partial f}{\partial \mathbf{P}_g}$
Non-mechanical strain	$\frac{dE^{nm}_{g,\,i}}{dt} = \begin{cases} \alpha \xi_r \left(-E^{nm}_{g,\,i} + aE_i\right) & \text{for} \quad \left\|aE_i\right\| > \left\|E^{nm}_{g,\,i}\right\| \\ \alpha \xi_r \left(-E^{nm}_{g,\,i} + E_i\right) & \text{for} \quad \left\|E_i\right\| < \left\|E^{nm}_{g,\,i}\right\| \end{cases}$

Table 1: Basic equation for elements in constitutive equation model

For calculating hyper elastic spring constants, Mooney-Rivlin equation requires some manipulation. Cauchy stress of SMP and SMPC is calculated as following equation (1). Assumption of calculating hyper elastic constants is that only hyper elastic components are working at high strain rate tensile test. Therefore, as shown equation (2), hyper elastic stretch can be calculated using total strain resulted from tensile test. Finally, equation (1) and equation (2) can be described as polynomial equation (3) at high strain rate tensile test. Also, hyper elastic constants can be obtained using linear fitting of equation (3).

$$\sigma_r = \frac{\left[2C^e_{10,r}\left\{(\lambda^e_r)^2 - \frac{1}{\lambda^e_r}\right\} + 2C^e_{01,r}\left\{\lambda^e_r - \frac{1}{(\lambda^e_r)^2}\right\}\right]}{\lambda^e_r \lambda^v_r} \tag{1}$$

$$\lambda = \lambda^e_r = 1 + \varepsilon \tag{2}$$

$$\frac{\lambda^{e2}_r \sigma_r}{2\left\{(\lambda^e_r)^2 - \frac{1}{\lambda^e_r}\right\}} = (\lambda^e_r C^e_{10,r} + C^e_{01,r}) \tag{3}$$

Equation (4) to Equation (11) are used to calculate the constant values of viscoelastic. The characteristic of viscoelastic is expressed as ordinary differential equation using the Mooney-Rivlin governing equations as shown in Equation (4). For calculating viscoelastic dashpot constants, the ordinary differential equation requires some manipulation. Assumption of calculating viscoelastic dashpot constant is that only viscoelastic components are working at constant stress condition and only hyper elastic components are working at instantaneous stress increment. Therefore, when creep test is applied, the only hyper elastic stretch is not working until the start of constant stress. After constant stress is maintained, only viscoelastic stretch is working. Using these assumptions, dashpot value of viscoelastic can be calculated using equation (8). And hyper elastic stretch and viscoelastic stretch can be obtained by the results of creep test. Finally, equation (4) can be described as polynomial equation (11) at creep test. Also, the viscoelastic constants can be obtained using linear fitting of equation (11).

$$\frac{d\lambda^v_r}{dt}[2(\lambda^v_r)^3 + \frac{1}{(\lambda^v_r)^3}] = \frac{1}{2}\frac{1}{\kappa_r}\left[h(C^e_{10,r}, C^e_{01,r}, \lambda^e_r) - h(C^v_{10,r}, C^v_{01,r}, \lambda^v_r)\right] \tag{4}$$

$$h(C^e_{10,r}, C^e_{01,r}, \lambda^e_r) = 2C^e_{10,r}\left\{(\lambda^e_r)^2 - \frac{1}{\lambda^e_r}\right\} + 2C^e_{01,r}\left\{\lambda^e_r - \frac{1}{(\lambda^e_r)^2}\right\} \tag{5}$$

$$h(C^v_{10,r}, C^v_{01,r}, \lambda^v_r) = 2C^v_{10,r}\left\{(\lambda^v_r)^2 - \frac{1}{\lambda^v_r}\right\} + 2C^v_{01,r}\left\{\lambda^v_r - \frac{1}{(\lambda^v_r)^2}\right\} \tag{6}$$

$$\kappa_r = \frac{1}{6}\frac{1}{\frac{d\lambda^v_r}{dt}}\left[h(C^e_{10,r}, C^e_{01,r}, \lambda^e_r)\right] \tag{8}$$

$$h(C^v_{10,r}, C^v_{01,r}, \lambda^v_r) = h\left(C^e_{10,r}, C^e_{01,r}, \lambda^e_r\right) - 2\kappa_r \frac{d\lambda^v_r}{dt}[2(\lambda^v_r)^3 + \frac{1}{(\lambda^v_r)^3}] \tag{9}$$

$$h(C^v_{10,r}, C^v_{01,r}, \lambda^v_r) = 2\left\{(\lambda^v_r)^2 - \frac{1}{\lambda^v_r}\right\}(C^v_{10,r} + \frac{1}{\lambda^v_r}C^v_{01,r}) \tag{10}$$

$$\frac{[h\left(C^e_{10,r}, C^e_{01,r}, \lambda^e_r\right) - 2\kappa_r \frac{d\lambda^v_r}{dt}\{(\lambda^v_r)^3 + \frac{1}{(\lambda^v_r)^3}\}]\lambda^v_r}{2\left\{(\lambda^v_r)^2 - \frac{1}{\lambda^v_r}\right\}} = (\lambda^v_r C^v_{10,r} + C^v_{01,r}) \tag{11}$$

2.2 Optimization process

Fig.2 shows the strategy to optimize the material constants obtained in the previous section. For the iteration process, the initial values of the material parameters were chosen as the results of previous section. In each iteration, the object function between simulated and experimental result for whole

testing time was calculated. When the object function was found to be minimum point, the iteration process was stopped. Using these sequence, the optimized material parameters of SMP can be obtained.

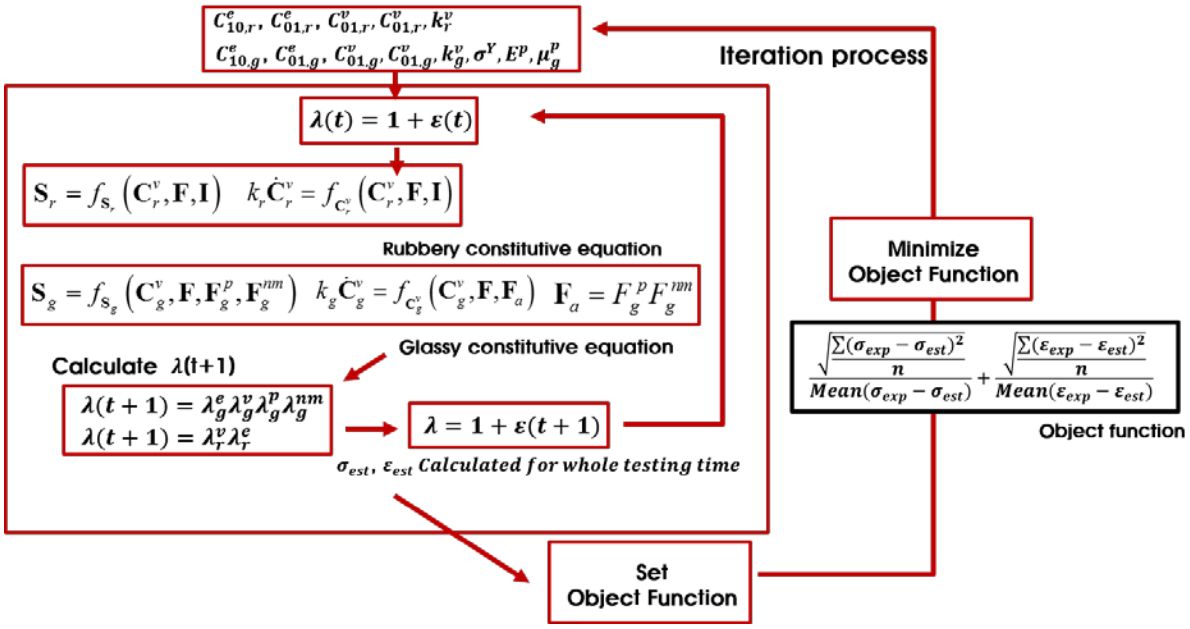

Figure 2: The schematic diagram for optimizing material parameters

2.2 Micro-level simulation

The finite element model to simulate the CNT-SMPCs has four distinct steps, (1) modelling geometry of the unit cell model, (2) defining the SMP matrix properties, (3) defining the CNT filler, and (4) defining the interface between CNT and SMP matrix. Fig. 3 shows the unit cell model to simulate CNT-SMP on micro scale. SMP resin was considered as homogenous and thus described by governing equation as mentioned in the previous section 2.1. CNT was considered as perfect elastic material. The density of CNT is 1.29g/cm^3 [5]. The interface between CNT and SMP resin are considered as perfect bonding in this paper. The mechanical simulation of CNT-SMPCs will be carried out and reported in detail at the conference.

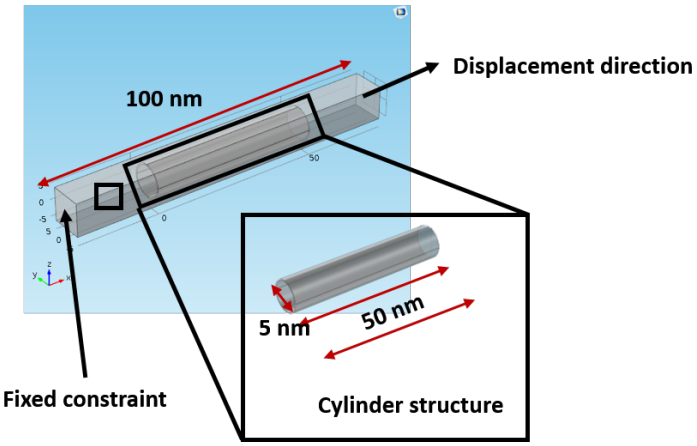

Figure 3: Unit cell model to simulate CNT-SMPCs

3 EXPERIMENT

3.1 Materials and fabrication

CNT-SMPCs are prepared using a SMP resin and multi-walled carbon nanotube(MWCNT). Epofix® resin and Jeffamine® D-230 are used for the thermoset SMP resin. The epoxy resin for shape memory polymer was Epofix® forming Structure and Jeffamine® D-230 from Huntsman was used as curing agent. The weight ratio of resin, curing agent and MWCNT was set to be 7:2:0.5. MWCNT and SMP

resin are mixed via tip sonication method. The mixture is cast on a hot mold in 130 ℃ for 8 hrs. For the mechanical testing, the testing specimen is cut into dog-bone shape according to ASTM D638.

CNT-SMPC samples with the dog-bone shape were fabricated using mold casting and tip sonication method. MWCNT with ~ aspect ratio was chosen as reinforcement of SMPC. The schematic for the manufacturing of SMPC is illustrated in Fig.4.

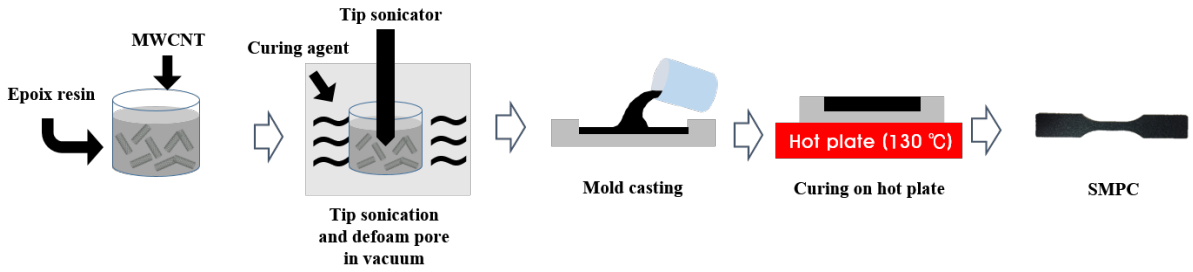

Figure 4: schematics for fabrication of CNT-SMPC

3.2 High strain rate tensile and creep test for mechanical properties of SMPC

For calculating viscoelastic and hyper elastic material parameters of rubbery and glassy phase, high strain rate tensile and creep test are conducted at each temperature using universal tensile machine with a heating chamber. 10 mm/min of crosshead speed was applied to perform the high strain rate tensile test. Fig.5 shows the picture of UTM and test specimen for tensile and creep test.

Figure 5: (a) Universal testing machine and (b) Testing specimen followed ASTM D638

3.2 Thermomechanical test for characterizing the shape memory behavior

3.2.1 Thermo-cycling test

The thermomechanical behavior of SMP and CNT-SMPC was characterized using UTM. One-way shape memory behavior was characterized in uniaxial tensile mode. The dynamic tensile mode with temperature condition of 20 ℃ to 120 ℃ was set.

The SMP specimen was deformed at 100 ℃, cooled down to 20 ℃ with keeping the deformation, and unloaded at 100 ℃with UTM in uniaxial tensile mode. The reason why SMP was reheated to 100

℃ is to measure the shape memory performance under stress free condition. Fig.5 shows testing procedure in shape memory test.

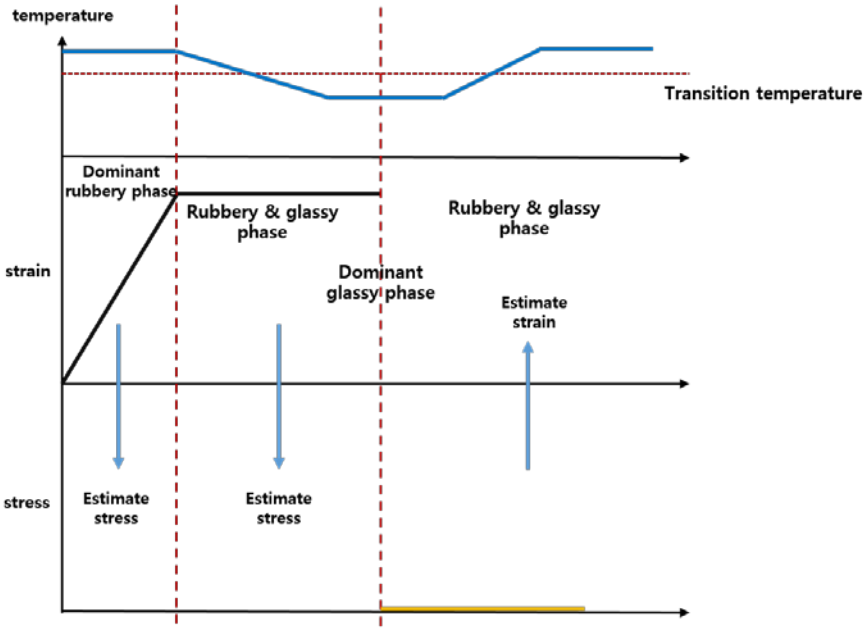

Figure 6: Testing procedure in shape memory test.

3.2.2 Isothermal mechanical test

For obtaining the material parameters of SMPs in rubbery state of the constitutive equation, rapid extension relaxation test was conducted at 100 ℃. The head speed was set to be 45mm/min. For obtaining the material parameters of SMPs in glassy state for the constitutive equation, slow extension-relaxation test was also conducted at 20 ℃ with the crosshead speed of 0.12 mm/min with UTM. The shape memory behavior of CF-SMPC was measured using uniaxial test.

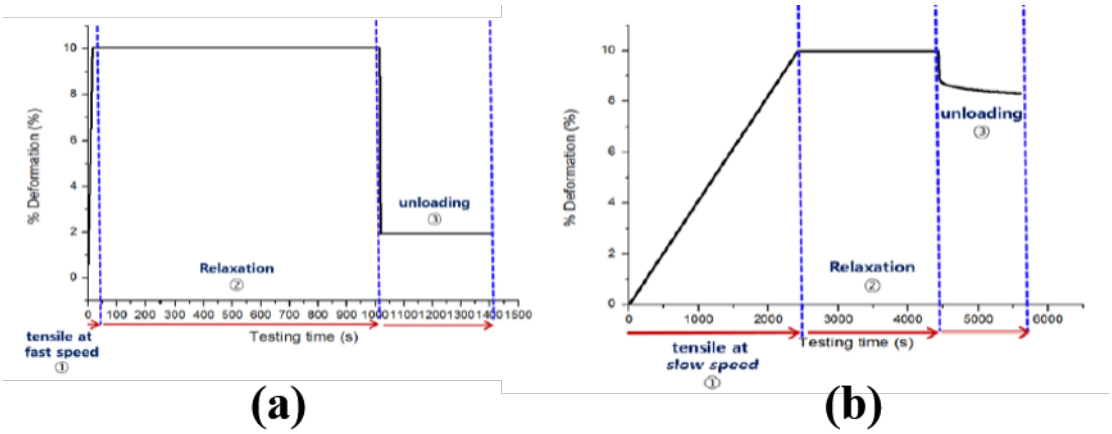

Figure 7: Isothermal mechanical test for (a) rubbery phase and (b) glassy phase

4 RESULTS AND DISCUSSION

4.1 Macro simulation results of CNT-SMPCs

The time-strain and time-stress behavior of the CNT-SMPCs are shown in Fig.8. Recovery and fixity rate of the CNT-SMPCs were calculated using equation (12) and (13).

$$Recovery\ ratio = \frac{\varepsilon_p - \varepsilon_r}{\varepsilon_p} \times 100(\%) \quad (12)$$

$$Fixity\ ratio = \frac{\varepsilon_f}{\varepsilon_p} \times 100(\%) \quad (13)$$

where ε_p was the strain when tensile stress applied to the specimen and ε_r was residual strain during recovery process. ε_f was the reduced strain during cooling process in fixing the specimen. The recovery and fixity ratio were 85.44 % and 91.43 %, respectively.

Using the test as mentioned in the previous section, the material parameters of CNT-SMPCs will be determined for the constitutive equation. The mechanical simulation results of CNT-SMPCs will be reported at the conference.

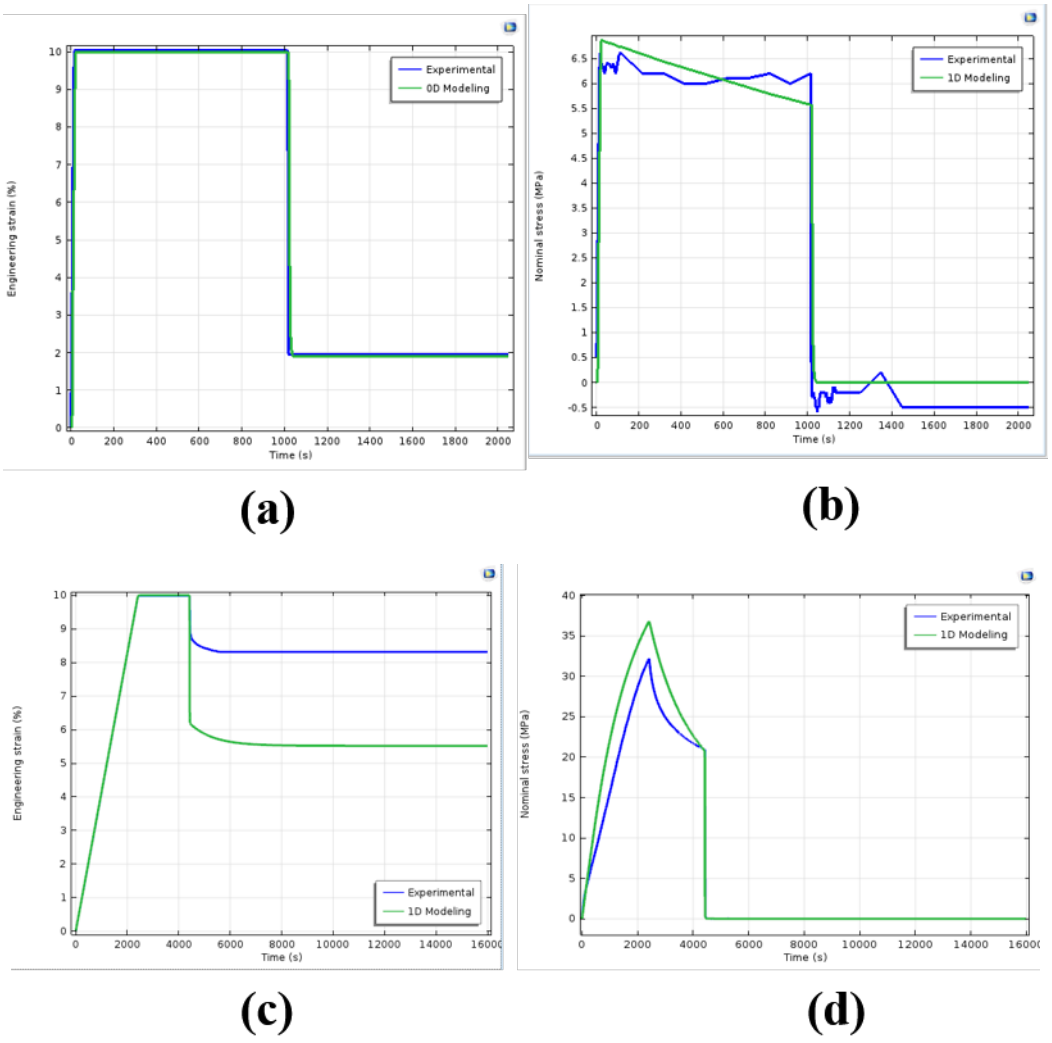

Figure 8: Simulation result for CNT-SMPCs (a) Time-strain simulation in 1D modeling at rubbery phase (b) Time-stress simulation in 1D modeling at rubbery phase (c) Time-strain simulation in 1D modeling at glassy phase (d) Time-stress simulation in 1D modeling at glassy phase

4.2 Micro simulation results of CNT-SMPCs

Before conducting micro simulation, characterization and analysis of SMP resin are needed for micro simulation of CNT-SMPCs. For SMP resin, the recovery and fixity ratio were 91.17 % and 73.77 %, respectively. The material parameters of SMP will be determined through the optimization process. For CNT filler, CNT was considered as perfect elastic material and the properties of CNT was used followed by the reference. Interface properties will be discussed at the conference and also simulation results of CNT-SMPCs will be reported at the conference.

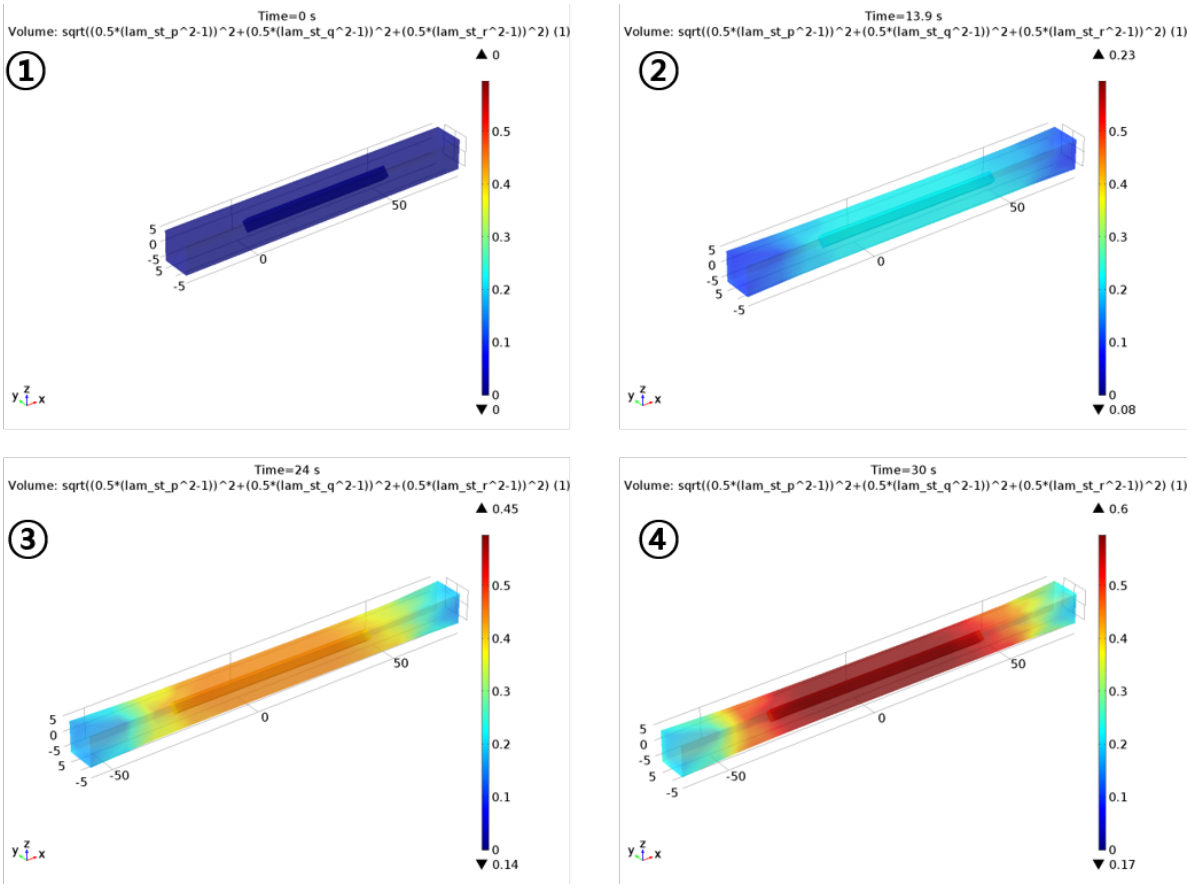

Figure 8: Simulation result of CNT-SMPCs unit cell model

5 CONCLUSIONS

The mechanical behaviour of CNT-SMPCs was analysed using 3D constitutive equation at macro and micro level. For macro level, the mechanical behavior of CNT-SMPC was characterized using various experiments and its deformation behavior was simulated using a three-dimensional constitutive model. For micro level simulation of CNT-SMPCs, SMP resin was considered as homogenous system while CNT filler was modelled as perfect elastic material. Detailed discussion on the interface modelling and simulation results will be provided at the conference.

ACKNOWLEDGEMENTS

This work was supported by Agency for Defense Development as a collaborative preliminary core technology research project.

REFERENCES

[1] Park, H., Harrison, P., Guo, Z., Lee, M. G., & Yu, W. R. (2016). Three-dimensional constitutive model for shape memory polymers using multiplicative decomposition of the deformation gradient and shape memory strains. Mechanics of Materials, 93, 43-62.

[2] Hong, S. B., San Ahn, Y., Jang, J. H., Kim, J. G., Goo, N. S., & Yu, W. R. (2016, April). Mechanical analysis of carbon fiber reinforced shape memory polymer composite for self-deployable structure in space environment. In SPIE Smart Structures and Materials+ Nondestructive Evaluation and Health Monitoring (pp. 98000S-98000S). International Society for Optics and Photonics.

[3] Chen, Y.-C. and D.C. Lagoudas, A constitutive theory for shape memory polymers. Part I: Large deformations. Journal of the Mechanics and Physics of Solids, 2008. 56(5): p. 1752-1765

[4] Chen, Y.-C. and D.C. Lagoudas, A constitutive theory for shape memory polymers. Part II: A linearized model for small deformations. Journal of the Mechanics and Physics of Solids, 2008. 56(5): p. 1766-1778.

[5] Jiang, L., Nath, C., Samuel, J., & Kapoor, S. G. (2014). Estimating the Cohesive Zone Model Parameters of Carbon Nanotube–Polymer Interface for Machining Simulations. Journal of Manufacturing Science and Engineering, 136(3), 031004.